

# Energy-efficient Coherent PON System with Access-span Length Difference between ONUs using Marginal IQ Power Loading in Downlink Transmission

Takahiro Kodama<sup>1,2</sup> and Kouki Arai<sup>3</sup>

1. Faculty of Engineering and Design, Kagawa University, 2217-20 Hayashi-cho, Takamatsu, Kagawa 761-0396, Japan
2. Department of Electrical, Electronics and Information Engineering, Osaka University, 2-1 Yamada-oka, Suita, Osaka 565-0871, Japan
3. Graduate Faculty of Interdisciplinary Research, University of Yamanashi, 4-3-11, Takeda, Kofu, Yamanashi 400-8511, Japan  
[tkodama@eng.kagawa-u.ac.jp](mailto:tkodama@eng.kagawa-u.ac.jp)

**Abstract:** 2.7 dB power efficiency improvement consistent with theory was experimentally obtained by marginal IQ distorted QPSK signal with and DD-CPR in the case of the 57 km downlink access span length difference between two ONUs.

© 2020 Takahiro Kodama and Kouki Arai

## 1. Introduction

Digital coherent technologies have been commercially used in long-reach optical communications, such as core and metro networks [1,2]. Digital coherent technologies commoditize; hence, they have shifted to short-reach optical communications, such as optical access and inter-datacenter networks [3-8]. As a feature of the digital coherent technology, the modulation degree has two advantages: it can be increased by using two orthogonal bases of the IQ channels, and the receiver sensitivity can be improved using the local light at the receiver side. Therefore, a 10 GSymbol/s/ $\lambda$  coherent passive optical network (PON)-based optical access system with digital coherent technology can be operated in large capacity per wavelength compared to the standardized 10 GPON system [9] and the time and wavelength division multiplexing (TWDM)-PON system [10] with intensity modulation and direct detection.

In the coherent PON downlink transmission, time-division multiplexed IQ modulated stream signals are transmitted from the optical line terminal (OLT) to each optical node unit (ONU). When the transmission distance to the OLT is different for each ONU in downlink transmission, the transmission light source power must be set such that the longest-reach ONU satisfies the desired signal quality, such as the forward error code (FEC) limit. As a result, the shortest-reach ONU receives excessive received power, and the power consumption during the system operation is wasted. Moreover, the conventional coherent system has a fixed-capacity transmission for each ONU; hence, adaptive resource management is required for dynamic capacity transmission.

We propose IQ mapping that makes the variable transmission rate and IQ imbalance modulation that optimizes the power of each axis according to the downlink transmission distance difference for the two ONUs to simultaneously solve the two abovementioned problems. The chromatic dispersion that causes signal distortion by short-reach transmission must be completely compensated by an equalizer at the receiver-side digital signal processing (DSP) to optimize IQ power loading for two ONUs with different distances to the OLT. In addition, fiber nonlinear effects are not observed in a short-reach transmission of less than a 70 km standard single mode fiber (SMF). However, a fourth-power-low-based Viterbi-and-Viterbi (VV) carrier phase recovery (CPR) limits setting IQ power ratio [11]; hence, the transmission distance difference between two ONUs that can be optimized has a limit [12]. A decision-directed (DD) CPR is proposed to accurately operate CPR for a non-regular quadrature-phase shift keying (QPSK) signal [13].

The present study proposes further reduction of power consumption in the downlink of the 10 GSymbol/s/ $\lambda$ , IQ imbalanced QPSK transmission in coherent PON system. The proposed scheme is applied for a single wavelength to confirm the principle operation. Using DD-CPR that can increase the setting IQ power ratio compared with the conventional VV-CPR widens the transmission distance difference between two ONUs that can be optimized. In the conventional VV-CPR, the setting IQ power ratio is limited from 0.6 to 1.7, whereas the DD-CPR can expand the setting IQ power ratio from 0.2 to 5.6. We numerically show that the power consumption can be reduced by 2.7 dB compared with the case of using the conventional balanced QPSK signal when the transmission distance difference between two ONUs is 57 km. We also numerically and experimentally demonstrate the effectiveness of DD-CPR on the IQ imbalanced QPSK signal.

## 2. CPR effects for IQ distorted QPSK signal

In the case of using the commercialized micro-integrated tunable laser assembly ( $\mu$ -ITLA), the signal light and the local light emission operate with a maximum deviation of  $\pm 1.5$  GHz with respect to the set center frequency [14]. Therefore, when the frequency offset is large, the CPR and the frequency offset compensation (FOC) such as a pre-

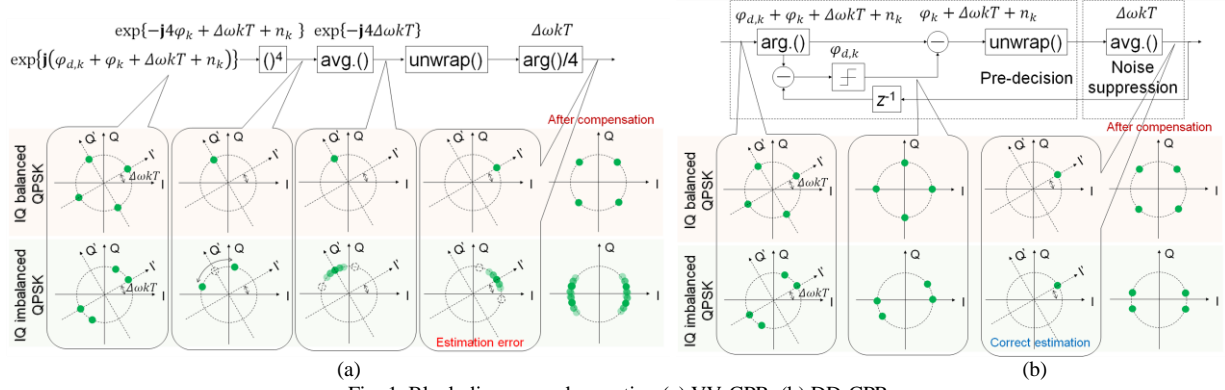


Fig. 1. Block diagram and operation (a) VV-CPR, (b) DD-CPR.

Table 1. Parameters

Symbol rate [GSymbol/s]	10
ADC sampling rate [GSa/s]	20
Dispersion parameter [ps/nm/km]	17
Fiber loss [dB/km]	0.2
LD center wavelength [nm]	1550
Received SNR [dB]	10

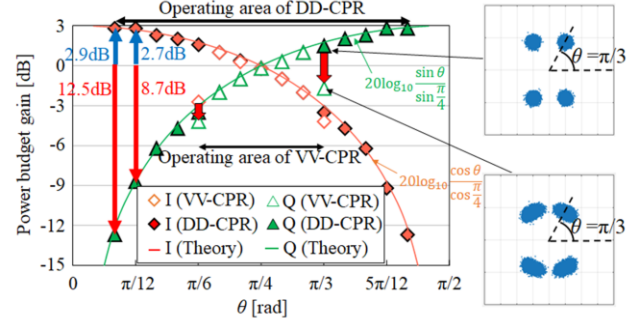


Fig. 2. Power-budget gain of IQ-imbalance.

decision-based angle difference estimation (PADE) are required. Figure 1(a) shows a block diagram and operation of VV-CPR. The  $k$ th received symbol is represented as  $\exp\{j(\varphi_{d,k} + \varphi_k + \Delta\omega kT + n_k)\}$ , where  $\varphi_{d,k}$  is the  $k$ th data, and its value is either  $\pm\pi/4$  or  $\pm 3\pi/4$ .  $\varphi_k$  is the  $k$ th carrier phase caused by the laser phase noise.  $\Delta\omega kT$  is a frequency offset value.  $T$  is the one symbol time.  $n_k$  is white Gaussian noise. The change of  $\Delta\omega$  within one cycle in the VV-CPR is small; hence,  $\Delta\omega kT$  is assumed constant. The phase component is all  $-1$  after the fourth power of  $\varphi_{d,k}$ . The noise is suppressed by averaging, and  $\exp(j4\varphi_k)$  is output. An estimated carrier frequency offset  $\Delta\omega kT$  is obtained after calculating  $\arg(\cdot)/4$ . Accordingly,  $\varphi_{d,k} = \pi/4$  when the power ratio is set to 1. The value becomes  $\pi(-1)$  after the fourth power. Therefore, VV-CPR can correctly estimate  $\Delta\omega kT$ . In contrast,  $\varphi_{d,k}$  is  $\pm\pi/6$ ,  $\pm 5\pi/6$  when the power ratio is set to 0.58. The value becomes  $\pm 4\pi/6$ , which is not  $-1$ , after the fourth power. Therefore, VV-CPR cannot accurately estimate  $\Delta\omega kT$ .

Figure 1(b) shows a block diagram and operation of DD-CPR. The phase  $\varphi_{d,k} + \varphi_k + \Delta\omega kT$  of the received signal is obtained by  $\arg(\cdot)$ . At the pre-decision part, estimated data  $\varphi_{d,k}$  are obtained by pre-decision using the previous estimated phase error  $\varphi_{k-1}$ .  $\varphi_{d,k}$  is subtracted from the received signal  $\varphi_{d,k} + \varphi_k + \Delta\omega kT + n_k$  to obtain  $\varphi_k + \Delta\omega kT + n_k$ . The noise is suppressed by averaging, and an estimated carrier phase  $\Delta\omega kT$  is obtained.

Table 1 shows the details of the simulation parameters. Figure 2 depicts the gain characteristics of the IQ components with respect to  $\theta$ , which is an index of the IQ imbalance in the IQ imbalanced QPSK signal. The gain characteristic was calculated based on the SNR when the bit error rate (BER) achieved  $10^{-3}$  under the condition that the frequency offset was fixed at 1 GHz. We confirmed that the VV-CPR operated only in the range of  $\pi/6 \leq \theta \leq \pi/3$ , whereas the DD-CPR operated at  $\pi/18 \leq \theta \leq 4\pi/9$ . In the case of  $\theta = \pi/3$ , DD-CPR is correctly operated as shown in Fig. 2. In contrast, VV-CPR is not correctly operated, and the expected power-budget gain cannot be obtained as shown in Fig. 2. In the case of  $\theta = \pi/18$ , a gain of 2.9 dB was obtained for the I channel, whereas a penalty of 12.5 dB happened for the Q channel. Accordingly, 2.9 dB power consumption can be reduced when the IQ imbalanced QPSK with IQ mapping was applied to a downlink system with a transmission distance difference of 77.5 km between two ONUs corresponding to a required SNR difference between the IQ channels of 15.5 dB.

### 3. Experimental setup and results

Figure 3 shows the experimental setup of the 10 GSymbol/s/ $\lambda$ ,  $\theta = \pi/12$ , IQ imbalanced QPSK-based PON downlink system using PADE and DD-CPR for FOC. We set the total SMF transmission lengths for ONU#1 and #2 to 0 km

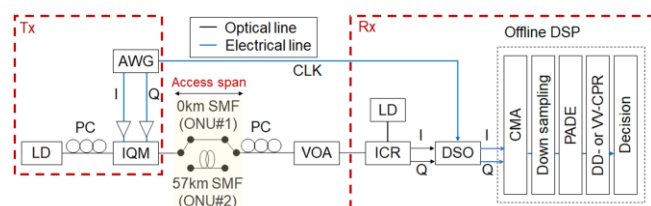


Fig. 3. Experimental setup.

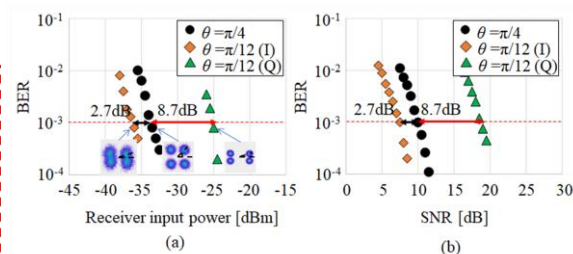


Fig. 4. (a) Experimental BERs, (b) numerical BERs.

and 57 km, respectively, to prove the concept behind the proposed method in an experiment with different access span lengths. As a proof-of-principle experiment, we assumed the IQ imbalanced signal generation and detection by an arbitrary waveform generator (AWG: Tektronix, 7122C) and a digital storage oscilloscope (DSO: Tektronix, 6154C). The sampling rates in AWG and DSO were 10 GSa/s and 20 GSa/s, respectively. The transmission fiber loss and dispersion were 0.2 dB/km and 17 ps/nm/km, respectively.

At the transmitter (Tx) side of the OLT,  $\theta$  was adjusted by alternating the power ratio of the I and Q channels using the IQ mapper to optimize the two ONUs' power budgets. The bias voltage and driver amplitude values were set similar to the balanced QPSK signal. The power imbalanced IQ channel signal was input to an IQ modulator (IQM). The unmodulated light from a tunable laser diode (LD) with 100 kHz linewidth at 1550 nm was launched into the IQM, and a 10 GSymbol/s IQ imbalanced QPSK signal was generated. The IQ imbalanced QPSK signal was launched into 0 km or 57 km of SMF as the access-span fiber.

At the receiver (Rx) side of each ONU, the signal power was adjusted by a variable optical attenuator (VOA) mixed with the local oscillator light and coherently detected. The detected signal was sampled and quantized by DSO. At the offline processing part, a constant modulus algorithm (CMA) was used to compensate for the effects of chromatic dispersion and spectral narrowing caused by the spectral characteristic of analog devices. After CMA, down sampling was processed from 20 GSa/s to 10 GSa/s. The down-sampled signal was processed by PADE and DD-CPR. The CMA was used to set the tap coefficient of a finite impulse response (FIR) filter with 15 taps. The step size parameter was 1/700. The average block size of DD-CPR was 31. The separate IQ channels were de-mapped, and the BERs for each ONU's signal were measured.

Figure 4(a) depicts the experimentally measured BER versus receiver input power when using IQ balanced and imbalanced modulation. In the case of balanced QPSK modulation, the receiver sensitivities of the ONUs were  $-33.5$  dBm. In the case of imbalanced QPSK modulation ( $\theta = \pi/12$ ), the receiver sensitivities of the ONUs were  $-36.2$  dBm and  $-24.8$  dBm. A gain of 2.7 dB was obtained for the I channel, whereas a penalty of 8.5 dB was happened for the Q channel. Therefore, we confirmed that the total transmission power can be reduced by 2.7 dB compared to the balanced QPSK case. The constellation maps were shown in the case of  $\text{BER} = 10^{-3}$ .

Figure 4(b) shows the numerical measured BER versus signal-to-noise ratio (SNR) when using IQ balanced and imbalanced modulation. As with the experimental results, the power budget of ONU#2, which had a longer reach, was improved by 2.7 dB when  $\theta$  was set to  $\pi/12$ . The BER of ONU#1, which had a shorter reach, satisfied the FEC limit. Therefore, the same low-power consumption effect was confirmed by the numerical and experimental results.

#### 4. Conclusions

We experimentally demonstrated a 2.7 dB power-budget improvement for the longer-reach ONU at 10 Gbit/s per ONU in the case of a 57 km SMF transmission distance difference with two ONUs' optimized power budgets. Since there is no penalty between the experimental result and the theoretical value, nonlinear effects do not become a problem in this verification, and a design based on the theory can be performed.

*We would like to thank T. Miyazaki and M. Hanawa of the University of Yamanashi for their supports in the experiment. This research is supported by the Okawa Foundation for Information and Telecommunications.*

#### References

- 1 K. Kikuchi, *JLT* **34**(1), 157-179, (2016).
- 2 S. J. Savory, *JSTQE* **16**(5), 1164-1179, (2010).
- 3 N. Suzuki et al., *JLT* **35**(8), 1415-1421, (2017).
- 4 R. Koma et al., in *Proc. ECOC*, paper M1E.4, (2016).
- 5 G. Pandey et al., *Opt. & Quant. Ele.*, **47**(11), 3445-3453, (2015).
- 6 M. S. Faruk et al., *Phot. J.*, **10**(1), (2018).
- 7 J. D. Reis et al., *JLT* **32**(4), 729-735, (2014).
- 8 S. You et al., *Opt. Comm.* **435**(15), 41-45, (2018).
- 9 K. Tanaka et al., *JLT* **28**(4), 651-661, (2010).
- 10 Y. Luo et al., *JLT* **31**(4), 587-593, (2013).
- 11 Z. Tao et al., *JSTQE* **16**(5), 1201-1209, (2010).
- 12 T. Kodama et al., in *Proc. OFC*, paper Th2A.22, (2017).
- 13 E. Ip et al., *JLT* **25**(9), 2675-2692, (2007).
- 14 T. Mukaiharu et al., in *Proc. OFC*, paper W1H.6, (2015).